Reynolds stress modelling of wall-bounded turbulent flows with an instability-sensitized closure

Suad Jakirlić* and Robert Maduta,†

Institute of Fluid Mechanics and Aerodynamics/Center of Smart Interfaces

Technische Universität Darmstadt, Petersenstr. 17, D-64287, Darmstadt, Germany

Abstract

Usually, a turbulence model designed and calibrated in the steady RANS (Reynolds-Averaged Navier-Stokes) framework has been straightforwardly applied to an unsteady calculation. It ended up in a steady velocity field in the case of confined wall-bounded flows; a somewhat better outcome is to be expected in globally unstable flows, such as bluff body configurations. However, only a weakly unsteady mean flow can be returned with the level of unsteadiness being by far lower compared to a referent database. Presently, an instability-sensitive, eddy-resolving model based on a differential, near-wall Reynolds stress model of turbulence is formulated and applied to several attached and separated wall-bounded configurations - channel and duct flows, external and internal flows separated from sharp-edged and continuous curved surfaces. In all cases considered the fluctuating velocity field was obtained started from the steady RANS results. The model proposed does not comprise any parameter depending explicitly on the grid spacing. An additional term in the corresponding length-scale determining equation providing a selective assessment of its production, modelled in terms of the von Karman length scale (comprising the second derivative of the velocity field) in line with the SAS (Scale-Adaptive Simulation) proposal (Menter and Egorov, 2010), represents here the key parameter.

1 Introduction

There has been a substantial activity in developing the hybrid LES/RANS methods and novel Unsteady RANS (URANS) methods (RANS model plays here the role of a subscale model). The relevant methods have been proposed by Spalart et al. (1997, DES - Detached Eddy Simulation; see Spalart, 2009 for the DES method upgrades, namely Delayed DES and Improved Delayed DES), Menter and Egorov (2010; SAS - Scale Adaptive Simulations), Girimaji (2006; PANS - Partially-Averaged Navier Stokes) and Chaouat and Schiestel (2005; PITM - Partially-Integrated Transport Model). The common feature of all these models is an appropriate modification of the scale-determining equation providing a dissipation rate level which

*Apl. Professor

†Doctoral student

suppresses the turbulence intensity towards the subgrid (i.e. subscale) level in the regions where large coherent structures with a broader spectrum dominate the flow, allowing in such a way evolution of structural features of the associated turbulence. Whereas an appropriate dissipation level enhancement in both PANS and PITM methods is achieved by reducing selectively (e.g. in the separated shear layer region) the destruction term in the model dissipation equation (i.e. its coefficient - e.g., the grid size-dependent model coefficient function in PITM method provides the decrease of the standard value $C_{\varepsilon,2} = 1.92$, prevailing in the near-wall region, towards the value $C_{\varepsilon,2} \approx 1.4$ in the separated shear layer of the periodic 2D hill flow, Jakirlic et al., 2009), an additional production term was introduced into the ω equation ($\omega \propto \varepsilon/k$ - inverse turbulent time scale) in the SAS framework. This term is modelled in terms of the von Karman lenght scale comprising the second derivative of the velocity field ($\nabla^2\mathbf{U}$), which is capable of capturing the vortex size variability, Menter and Egorov (2010).

The work reported here aims at developing an instability sensitive, anisotropy-resolving Second-Moment Closure (SMC) model. This model scheme, functioning as a 'sub-scale' model in the Unsteady RANS framework, represents a differential near-wall Reynolds stress model formulated in conjunction with the scale-supplying equation governing the homogeneous part of the inverse turbulent time scale: $\omega_h = \varepsilon_h/k$. The model capability to account for the vortex length and time scales variability was enabled through a selective enhancement of the production of the dissipation rate in line with the SAS proposal (Scale-Adaptive Simulation, Menter and Egorov, 2010) pertinent particularly to the highly unsteady separated shear layer region. For more detailed insight into the modeling rationale and computational issues interested readers are referred to the original references. The predictive performances of the proposed model are checked by computing series of internal and external, two-dimensional and three-dimensional flows in channels, ducts and past bluff bodies including separation from sharp-edged and continuous curved surfaces in a range of Reynolds numbers.

2 Computational method

The equation governing the homogeneous part of the total viscous dissipation rate, $\varepsilon_h = \varepsilon - 0.5\nu\partial^2 k/(\partial x_j \partial x_j)$, modelled in term-by-term manner by Jakirlic and Hanjalic (2002) represents the starting point for the present development. The RSM-based ω_h-equation following directly from the ε_h-equation (here, instead of originally used General-Gradient-Diffusion-Hypothesis (GGDH) for the turbulent diffusion modelling, the Simple GDH with diffusion coefficient modelled in terms of turbulence viscosity was applied; thereby, no difference between the Prandtl-Schmidt numbers corresponding to the quantities k and ε_h was made; one adopted finally $\sigma_\omega = \sigma_\varepsilon = 1.1$) by using well-known relationship

$$\frac{\mathbf{D}\omega_h}{\mathbf{D}t} = \frac{1}{k}\frac{\mathbf{D}\varepsilon_h}{\mathbf{D}t} - \frac{\varepsilon_h}{k^2}\frac{\mathbf{D}k}{\mathbf{D}t} \tag{1}$$

reads:

$$\begin{aligned}\frac{\mathbf{D}\omega_h}{\mathbf{D}t} = & \frac{\partial}{\partial x_k}\left[\left(\frac{1}{2}\nu + \frac{\nu_t}{\sigma_\omega}\right)\frac{\partial \omega_h}{\partial x_k}\right] - (C_{\varepsilon,1} - 1)\frac{\omega_h}{k}\overline{u_i u_k}\frac{\partial U_i}{\partial x_k} - (C_{\varepsilon,2} - 1)\omega_h^2 \\ & + \frac{2}{k}\left(\frac{1}{2}\nu + \frac{\nu_t}{\sigma}\right)\frac{\partial \omega_h}{\partial x_k}\frac{\partial k}{\partial x_k} + \frac{1}{k}P_{\varepsilon,3}\end{aligned} \tag{2}$$

where $P_{\varepsilon,3}$ represents the gradient production term (modelled by using the vorticity transport theorem) comprising both the mean rate of strain and second derivative of the velocity field.

The model for turbulent viscosity ν_t, accounts for both Reynolds stress anisotropy (beyond the reach of the eddy-viscosity model group) and viscosity effects, with characteristic length representing a switch between the Kolmogorov length scale and the turbulent length scale.

The latter equation is appropriately extended through the introduction of the SAS term (Menter and Egorov, 2010) into the ω_h-equation:

$$\frac{\mathbf{D}\omega_{h,SAS}}{\mathbf{D}t} = \frac{\mathbf{D}\omega_h}{\mathbf{D}t} + P_{SAS}; \quad P_{SAS} = C_{RSM,1}\max\left[P^*_{SAS}, 0\right]$$

$$P^*_{SAS} = 1.755\kappa S^2\left(\frac{L}{L_{vk}}\right)^{\frac{1}{2}} - 3k\max\left(C_{RSM,2}\frac{(\nabla\omega_h)^2}{\omega_h^2}, \frac{(\nabla k)^2}{k^2}\right) \tag{3}$$

with $L = k^{1/2}/\omega_h$ being the turbulent length scale, $L_{vk} = \max(\kappa S/|\nabla^2 U|; C_{RSM,3}\Delta)$ ($\Delta = (\Delta_x\Delta_y\Delta_z)^{1/3}$) representing the 3-D generalization of the classical boundary-layer definition of the von Karman length scale and S the invariant of the mean strain tensor ($S = \sqrt{2S_{ij}S_{ij}}$). It should be noted that the P_{SAS} term introduced in the ω_h-equation has almost identical form as the one being used in the eddy-viscosity-based $k-\omega$ SST-SAS model (Menter and Egorov, 2009). However, two coefficients, $C_{RSM,1} = 0.008$ and $C_{RSM,2} = 8$, reducing appropriately the intensity of the term, are introduced in order to adjust its use in the framework of a Second-Moment Closure model (it should be noted, that the coefficients $C_{\varepsilon,1}$ and $C_{\varepsilon,2}$ retained their standard values 1.44 and 1.92 respectively). Herewith, the RANS function of the present method is preserved within the near-wall region. The natural decay of the homogeneous isotropic turbulence, fully-developed channel flows in a range of Reynolds number (with underlying velocity field following the logarithmic law) and the non-equilibrium 2-D hill flow at two different Reynolds numbers ($Re_H = 10600$ and 37000) have been interactively computed in the process of the coefficients calibration. The limiter $C_{RSM,3}\Delta$ in the L_{vk}-formulation, originally introduced by Menter and Egorov (2010), aims primarily at capturing correctly the turbulence spectra behaviour in the decay process of the homogeneous isotropic turbulence focussing in particular on the high-frequency range. However, this addition does not play important role in the wall-bounded flow configurations.The contours of the P_{SAS} term depicted in Fig. 1 clearly shows that it is active only in the region of the separated shear layer. In the reminder of the flow domain, especially in the near-wall regions, its effect vanishes.

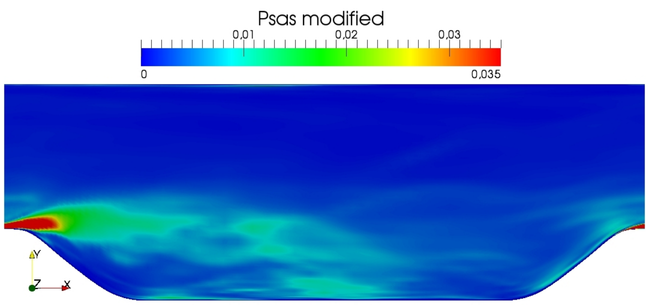

Figure 1: Magnitude of the P_{SAS} term (Eq. 3) in the 2D hill flow

All computations were performed using the code Open-FOAM (Weller et al., 1998, see also www.opencfd.co.uk/openfoam), an open source Computational Fluid Dynamics toolbox, utilizing a cell-center-based finite volume method on an unstructured numerical grid and employing the solution procedure based on the implicit pressure algorithm with splitting of operators

(PISO) for coupling between pressure and velocity fields. SIMPLE procedure was applied when computing the steady flows using the RANS-SMC model. The convective transport was discretized by the so-called 'gamma scheme' (Jasak, 1996 PhD thesis, IC London), blending between 2nd order central differencing and 1st order upwind schemes with $\gamma_{CDS} = 0.95$ and $\gamma_{UDS} = 0.05$ in most of the cases computed. For the time integration the 2nd order three point backward scheme was used. The code is parallelized applying the Message Passing Interface (MPI) technique for communication between the processors.

For more detailed insight into the modeling rationale and computational issues interested readers are referred to the original references.

3 Results and discussion

The predictive performances of the proposed models are intensively assessed in numerous aerodynamic-type flows of different complexity featured also by 2D and 3D separation along with available experimental, DNS and LES reference results. Figures 2-8 display some selected results obtained by the consequent models application. For the sake of the mutual comparison the results of the "background" RANS-RSM model are also depicted. For more extensive result presentation and more detailed discussion interested readers should consult the original references (see the reference list).

4 Conclusion

Potential of an eddy-resolving scheme, representing a novel URANS model, was illustrated by computing a series of wall-bounded flow configurations featured by separation and reattachment in a broad range of Reynolds numbers. Promising results with respect to the structural characteristics of the instantaneous flow field, the mean velocity field and associated integral parameters (e.g., friction and pressure coefficients) as well as the turbulence quantities demonstrate the model feasibility and applicability in a broad range of complex turbulent flows.

Acknowledgments

The work of R. Maduta has been funded by the EU project ATAAC (ACP8-GA-2009-233710)

References

[1] Chaouat, B. and Schiestel, R.: "A new partially integrated transport model for subgrid-scale stresses and dissipation rate for turbulent developing flows". *Phys. Fluids*, Vol. 17 (065106), pp. 1-19, 2005

[2] Cherry, E.M., Elkins, C.J. and Eaton, J.K.: "Geometric sensitivity of three-dimensional separated flows". *Int. J. of Heat and Fluid Flow*, Vol. 29, pp. 803-811, 2008

[3] Fröhlich, J., Mellen, C.P., Rodi, W., Temmerman, L. and Leschziner, M.A.: "Highly resolved large-eddy simulation of separated flow in a channel with streamwise periodic constrictions". *J. Fluid Mech.*, Vol. 526, pp. 19-66, 2005

[4] Girimaji, S.S.: "Partially-Averaged Navier-Stokes Model for Turbulence: A Reynolds-Averaged Navier-Stokes to Direct Numerical Simulation Bridging Method". *Journal of Applied Mechanics*, Vol. 73, pp. 413-421, 2006

[5] Jakirlic, S. and Hanjalic, K.: "A new approach to modelling near-wall turbulence energy and stress dissipation". *J. Fluid Mech.*, Vol. 439, pp. 139-166, 2002

[6] Jakirlic, S., Saric, S., Kniesner, B., Kadavelil, G., Basara, B. and Chaouat, B.: "SGS modelling in LES of wall-bounded flows using transport RANS models: from a zonal towards a seamless hybrid LES/RANS method". 6th Int. Symp. on Turbulence and Shear Flow Phenomena (TSFP6), Seoul, Korea, June 22-24, 2009

[7] Jakirlic, S., Maduta, R. and Ullrich, M.: "Performance assessment of the Scale-adaptive Reynolds stress model by reference to tandem-cylinder configurations". 9th Int. Symp. on Eng. Turb. Modelling and Measurements (ETMM9), Thessaloniki, June 6-8, 2012

[8] Jovic, S. and Driver, D.: "Reynolds number effect on the skin friction in separated flows behind a backward-facing step". *Experiment in Fluids*, Vol. 18, pp. 464-467, 1995

[9] Le, H., Moin, P. and Kim, J.: "Direct Numerical Simulation of Turbulent Flow over a Backward-Facing Step". *J. Fluid Mech.*, Vol. 330, pp. 349-374, 1997

[10] Maduta, R. and Jakirlic, S.: "Sensitizing Second-Moment Closure model to turbulent flow unsteadiness". *Computational Fluid Dynamics 2010*, A. Kuzmin (Ed.), pp. 341-347, Springer Verlag (ISBN 978-3-642-17883-2), 2010

[11] Maduta, R. and Jakirlic, S.: "An eddy-resolving Reynolds stress transport model for unsteady flow computations". In "Advances in Hybrid RANS-LES Modelling 4". Notes on Numerical Fluid Mechanics and Multidisciplinary Design, Vol. 117, S. Fu et al. (Eds.), pp. 77-89, Springer Verlag, ISBN 978-3-642-31817-7, 2012

[12] Menter, F.R. and Egorov, Y.: "The Scale-Adaptive Simulation Method for Unsteady Turbulent Flow Predictions. Part 1: Theory and Model Description". *Flow, Turbulence and Combustion*, Vol. 85, pp. 113-138, 2010

[13] Moser, R.D., Kim., J. and Mansour, N.N.: "Direct numerical simulation of turbulent channel flow up to $Re_\tau = 590$". *Physics of Fluids*, Vol. 11(4), pp. 943-945, 1999

[14] Neuhart, D.H., Jenkins, L.N., Choudhari, M.M. and Khorrami, M.R.: "Measurements of the Flowfield Interaction between Tandem Cylinders". AIAA-2009-3275, 2009

[15] Ohlsson, J., Schlatter, P., Fischer P.F. and Henningson, D.S.: "DNS of separated flow in a three-dimensional diffuser by the spectral-element method". *J. Fluid Mech.*, Vol. 650, pp. 307-318, 2010

[16] Rapp, Ch. and Manhart, M.: "Flow over periodic hills: an experimental study". *Experiments in Fluids*, Vol. 51, pp. 247-269, 2011

[17] Spalart, P.R., Jou, W.-H., Strelets, M. and Allmaras, S.: "Comments on the feasibility of LES for wings and on a hybrid RANS/LES approach". 1st AFOSR Int. Conf. on DNS and LES, 1997

[18] Spalart, P.R.: Detached-Eddy Simulation. *Annu. Rev. Fluid Mech.*, Vol. 41:181-202, 2009

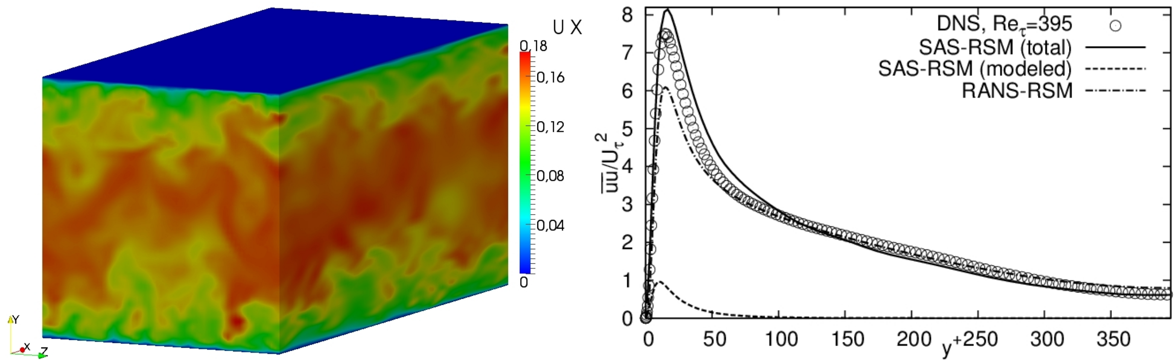

Figure 2: Fully-developed flow in a plane channel at $Re_\tau = 395$ - instantaneous axial velocity field obtained by SAS-RSM (left) and the streamwise Reynolds stress component (right); DNS from Moser et al. (1999).

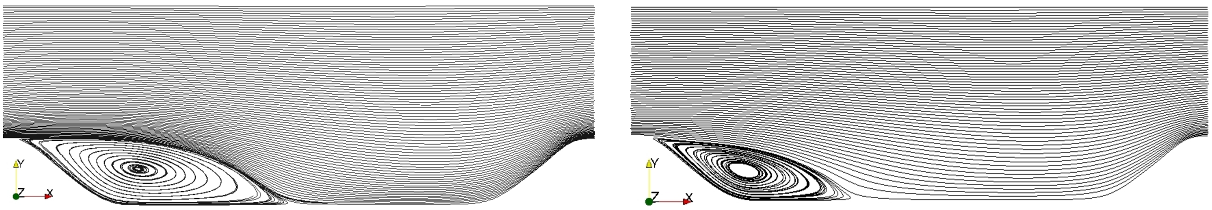

Figure 3: Periodic flow over a 2D hill at $Re_H = 10600$ (left) and $Re_H = 37000$ (right) - mean streamlines obtained by the SAS-RSM model.

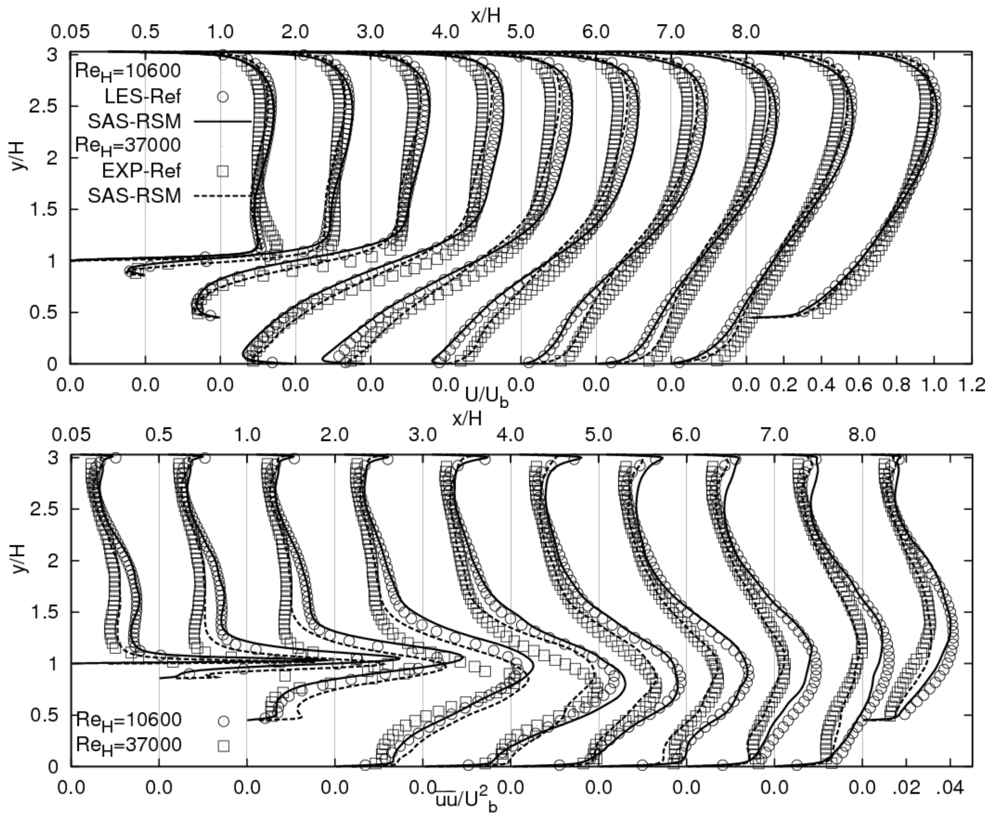

Figure 4: Periodic flow over a 2D hill - mean velocity and kinetic energy of turbulence profile developments obtained by the SAS-RSM model; Exp. from Rapp and Manhart, 2011; LES from Frölich et al., 2005

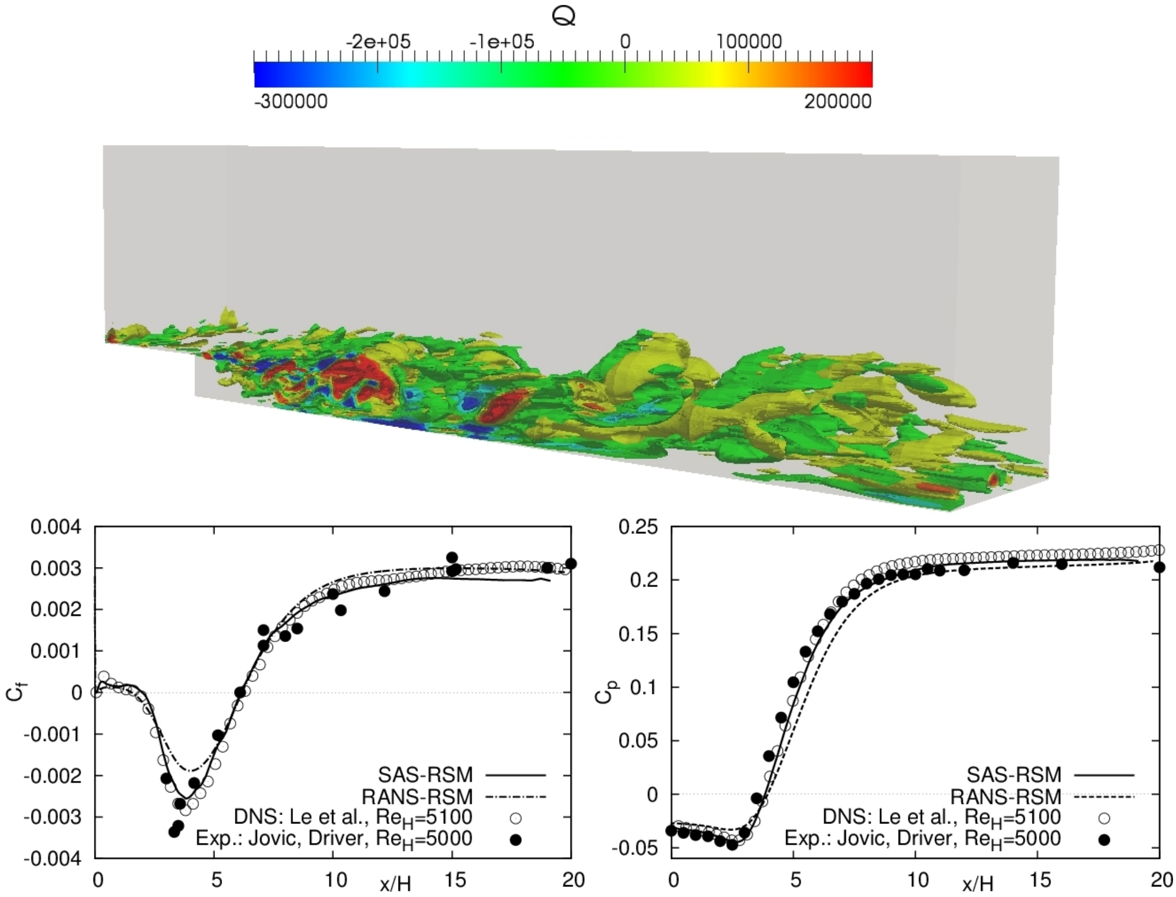

Figure 5: Flow over a backward facing step - vortex structure illustrated by the Q-criteria (upper), friction and pressure coefficients (lower)

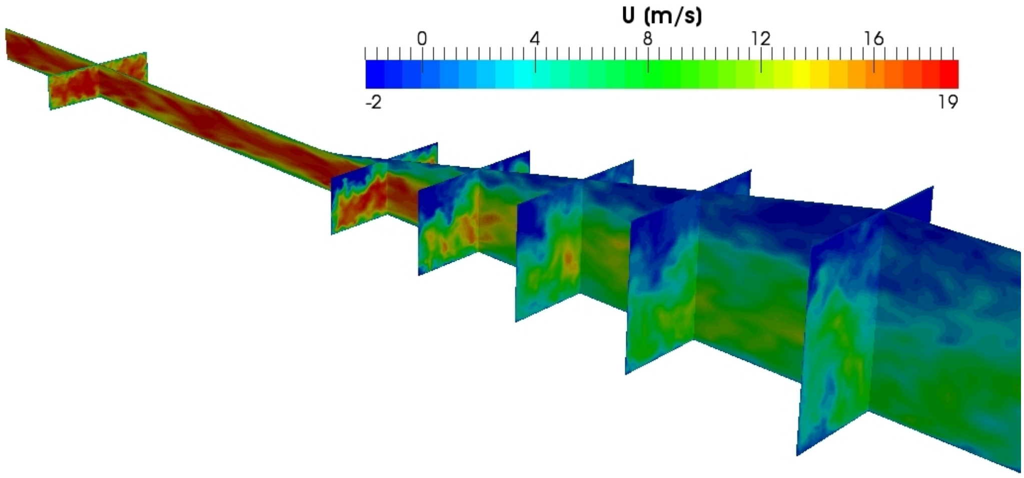

Figure 6: Flow in a three-dimensional diffuser - fully-developed flow in the inlet duct (height h=1 cm, width B=3.33 cm) expands into a diffuser: the upper-wall expansion angle is 11.3^o and the side-wall expansion angle is 2.56^o. Instantaneous velocity field, obtained by the present SAS-RSM model, illustrates the separation zone spreading over the entire upper wall.

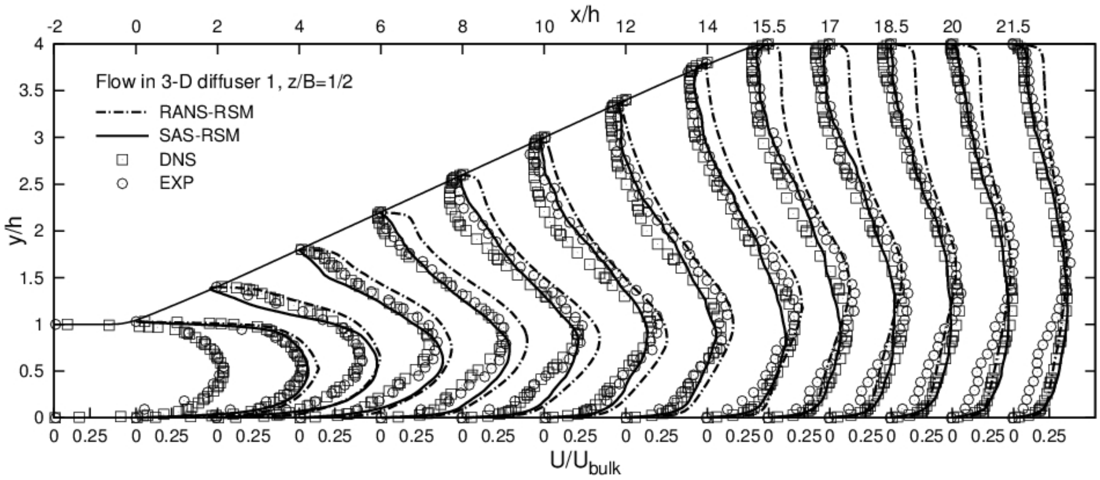

Figure 7: Flow in a three-dimensional diffuser - evolution of the axial velocity profile. Exp. from Cherry et al., 2008; DNS from Ohlsson et al., 2010

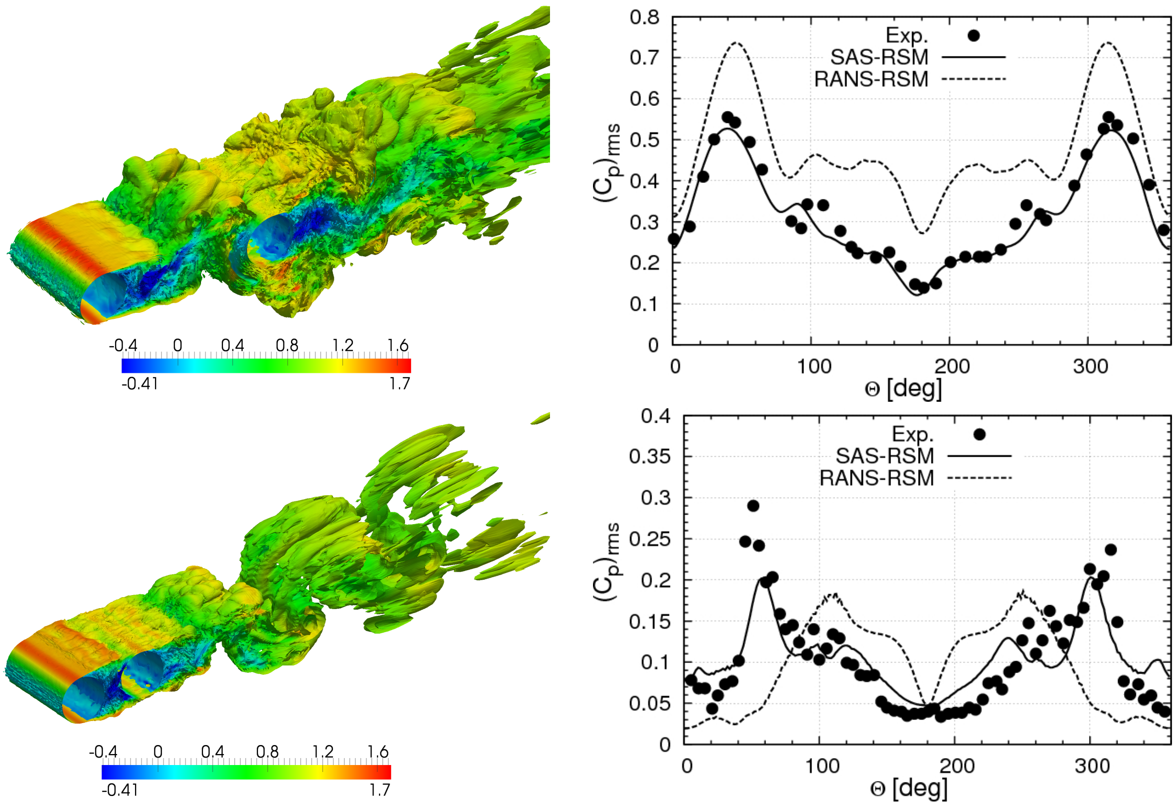

Figure 8: Flow past tandem cylinder configurations - large (L/D=3.7; upper) and small in-between spacing (L/D=1.435; lower); vorticity magnitude coloured by the normalized axial velocity (U_x/U_{inlet}) obtained by SAS-RSM (left) and root-mean-square (rms) of the fluctuating pressure on the downstream cylinder (right); Exp. from Neuhart et al., 2009